Topologically-based segmentation of brain structures from T1 MRI

Sanae Miri[1, 2], Nicolas Passat[1], Jean-Paul Armspach[2]

[1]Université Strasbourg 1, LSIIT, UMR 7005 CNRS/ULP, France
[2]Université Strasbourg 1, LINC, UMR 7191 CNRS/ULP, France

Introduction

Cerebral structure segmentation from 3D MRI data is an important task for several medical applications. Brain segmentation methods are primarily based on the classification of the intracranial volume into classes corresponding to the main cerebral tissues: cerebrospinal fluid (CSF), grey matter (GM), and white matter (WM). These classes present complex geometrical properties. However, they can be discriminated thanks to their distinct signal in modalities such as T1 or T2 MRI; moreover, the cerebral tissues present invariant and specific topological properties. Based on these assumptions, some topology-driven brain tissue classification techniques have been proposed [1,2,3]. The method described in this poster belongs to the same family of techniques, since its purpose is the classification of the brain into four classes: sulcal CSF, GM, WM, and ventricular CSF. These classes are modelled (with some simplifying hypotheses) as hierarchically included spheres. Starting from a presegmentation based on this model, the four classes then evolve under photometric constraints. This process can be formalised as a discrete multi-class deformable model.

Method

Input/output

The method takes as input a T1 MRI of the brain, $I : E \to \mathbb{N}$ (with $E = [0, d_x - 1] \times [0, d_y - 1] \times [0, d_z - 1]$, generally $[0, 255]^3$), from which the intracranial volume $E' \subset E$ has been extracted, (Fig. 1, 2nd picture), and two threshold values $\mu_1 < \mu_2 \in \mathbb{N}$ delimiting the T1 signal intensity between CSF/GM, and GM/WM, respectively. The method output is a partition $C = \{C_s, C_g, C_w, C_v\}$ of E', where C_s, C_g, C_w, and C_v correspond to the sulcal CSF, GM, WM, and ventricular CSF classes, respectively.

Initialisation

The method starts from a presegmentation C^i of E' having the desired topology: C^i_v is simply connected (1 connected component, 0 hole, 0 cavity), and successively surrounded by C^i_w, C^i_g, and C^i_s which are topological hollow spheres (1 connected component, 0 hole, 1 cavity), hierarchically organised, as illustrated in a 2D fashion in Fig. 1 (1st picture). In $\mathbb{Z}^3$, such a model implies to choose dual adjacencies for the successive classes. The 6-adjacency has been considered for C^i_g (and thus C^i_v), since GM is geometrically organised as a "thick" ribbon, while the 26-adjacency has been considered for C^i_w, C^i_v, since they both present thin details near the cortex. The initial presegmentation C^i is composed of a simply connected volume corresponding to C^i_v, surrounded by three "thick" closed surfaces, modelling C^i_w, C^i_g and C^i_s, their thickness corresponding to a coherent anatomical approximation (Fig. 1, 3rd picture).

Deformable process

From a topological point of view, C^i, although composed of four distinct classes, can be considered as a binary image constituted of an object $X = C^i_s \cup C^i_w$ and of the background $\overline{X} = C^i_g \cup C^i_v$, in a $(26, 6)$-adjacency framework. Based on this assumption, the segmentation process consists in modifying the frontier between X and $\overline{X}$ in a topology-preserving fashion, under photometric constraints. This discrete deformable model process is formalised in Alg. 1. It firstly modifies the classification of the points which are, from a photometric point of view, the "most misclassified". In order to preserve the topology of the initial model, only simple points [4] can be switched from a class to another. For simplicity's sake, the algorithm is presented using set-based notations. However, it was implemented using efficient data structures (ordered FIFO lists), enabling to reach an optimal algorithmic complexity $O(|E'|)$, linear w.r.t the size of the intracranial volume, since each point can be switched from one class to another only twice (the classification only depending on two threshold values).

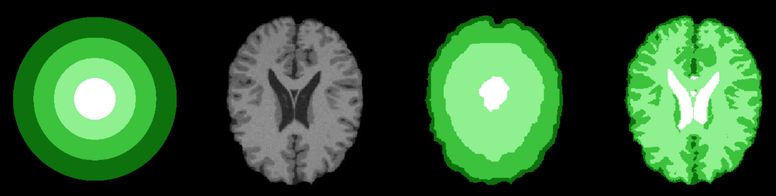

Fig. 1 - From left to right: topological model (from white to dark green: C^i_v, C^i_w, C^i_g, and C^i_s); T1 MRI ($I_{|E'}$: axial slice); initialisation of the segmentation process of the MRI (C_i); result of the segmentation (C).

repeat
1 - *Frontier point determination*
$FP_{\{s,g\}} = (C^i_s \cap N^*_6(C^i_g)) \cup (C^i_g \cap N^*_{26}(C^i_s))$
$FP_{\{g,w\}} = (C^i_g \cap N^*_{26}(C^i_w)) \cup (C^i_w \cap N^*_6(C^i_g))$
$FP_{\{w,v\}} = (C^i_w \cap N^*_6(C^i_v)) \cup (C^i_v \cap N^*_{26}(C^i_w))$
/* $N^*_k(A)$ is the set of points of $\overline{A}$ k-adjacent to A */
2 - *Simple point determination*
$SP_{26} = \{x \in X \mid x \text{ is 26-simple for } X\}$
$SP_6 = \{x \in \overline{X} \mid x \text{ is 6-simple for } \overline{X}\}$
3 - *Candidate point determination*
$CP = (SP_6 \cup SP_{26}) \cap (FP_{\{s,g\}} \cup FP_{\{g,w\}} \cup FP_{\{w,v\}})$
/* Simple points at the frontier between two classes */
4 - *Cost evaluation*
for all $x \in CP \cap FP_{\{s,g\}}$ (resp. $FP_{\{g,w\}}$, $FP_{\{w,v\}}$) **do**
$v(x) = I(x) - \mu_1$ (resp. $I(x) - \mu_2$, $I(x) - \mu_1$)
if $x \in C^i_g$ (resp. C^i_w, C^i_w) **then**
$v(x) = -v(x)$
end if
end for
5 - *Point selection and re-classification*
if $\max(v(CP)) > 0$ /* with $\max(v(\emptyset)) = -\infty$ */ **then**
Let $y \in CP$ such that $v(y) = \max(v(CP))$
Let $C^i_\alpha \in \{C^i_s, C^i_g, C^i_w, C^i_v\}$ such that $y \in C^i_\alpha$
Let $C^i_\beta \in \{C^i_s, C^i_g, C^i_w, C^i_v\}$ such that $y \in FP_{\{\alpha,\beta\}}$
$C^i_\alpha = C^i_\alpha \setminus \{y\}$
$C^i_\beta = C^i_\beta \cup \{y\}$
end if
until $\max(v(CP) \leq 0)$
$C = C^i$

Alg. 1 - Multi-class topology-preserving deformable process algorithm.

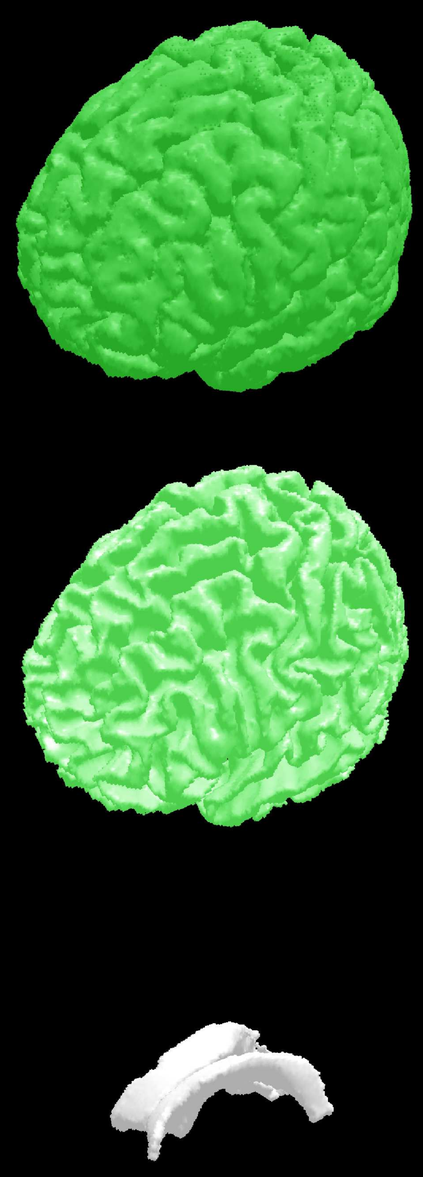

Fig. 2 - 3D visualisation of brain segmentation from a BrainWeb image, provided by the proposed method. From top to bottom: C_g (GM), C_w (WM), and C_v (ventricular CSF).

Results and discussion

An example of segmented image is available in Fig. 2. Depending on two parameters (μ_1 and μ_2), and relying on a linear complexity process, the proposed segmentation method enables to obtain results in a fast and easy way (computation time lower than 2 min. for a 256^3 image).
In order to validate the method, T1 MRI data provided by the commonly used BrainWeb database have been considered. BrainWeb enables to generate synthesis - but realistic - brain MRI data which are obtained from an anatomical ground truth by simulating the chosen MRI acquisition protocol (possibly integrating noise and artifacts).
The results obtained for images corresponding to noise ratios varying from 0% to 9% of corrupted voxels have been analysed by considering, for each class of tissue, three classical statistical measures: sensitivity ($TP/(TP + FN)$), specificity ($TN/(TN + FP)$) and similarity ($2.TP/(2.TP + FP + FN)$), with TN, TP, FN and FP corresponding to the number of true negative, true positive, false negative and false positive voxels, respectively. The obtained values of these measures are summarised in Tab. 1. The result illustrated in Fig. 2 corresponds to the measures of the first line (0% noise) of this table.

	Sensitivity (%)			Specificity (%)			Similarity (%)		
Noise	CSF	WM	GM	CSF	WM	GM	CSF	WM	GM
0%	88.5	99.4	81.5	99.4	98.2	99.8	83.6	91.8	89.0
1%	88.9	99.3	83.2	99.3	98.5	99.8	83.2	93.1	90.0
3%	89.7	95.4	85.9	98.9	99.6	99.4	79.8	95.7	90.4
5%	89.8	87.2	81.2	98.6	99.7	98.5	76.4	91.6	84.8
7%	90.0	80.0	75.9	98.3	99.6	97.7	74.0	87.1	79.2
9%	82.3	62.1	66.9	97.7	99.6	95.7	65.6	75.0	68.1

Tab. 1 - Sensitivity, specificity and similarity measures of segmentation results provided by the proposed method when applied on the BrainWeb database, for various noise ratios.

This method constitutes preliminary works, and is then not yet fully satisfying. The deformation process is only guided by photometric constraints, neglecting high-level anatomical knowledge such as volumetric or thickness information. Moreover, the initial topological model does not perfectly take into account structures such as the brainstem and the cerebellum, providing good results on the superior part of the brain (cortex), but less correct ones on its inferior part.
A more sophisticated version of the method, involving a presegmentation topologically and anatomically closer from the reality, and using both photometric and geometric constraints to guide the deformable model process is under development and will be further submitted for publication.

References

[1] J.-F. Mangin, V. Frouin, I. Bloch, J. Régis, J. López-Krahe. *From 3D magnetic resonance images to structural representations of the cortex topography using topology preserving deformations.* Journal of Mathematical Imaging and Vision, **5**(4):297–318, 1995.
[2] P. Dokládal, I. Bloch, M. Couprie, D. Ruijters, R. Urtasun, L. Garnero. *Topologically controlled segmentation of 3D magnetic resonance images of the head by using morphological operators.* Pattern Recognition, **36**(10):2463–2478, 2003.
[3] P.-L. Bazin, D.L. Pham. *Topology-preserving tissue classification of magnetic resonance brain images.* IEEE Transactions on Medical Imaging, **26**(4):487–496, 2007.
[4] G. Bertrand, G. Malandain. *A new characterization of three-dimensional simple points.* Pattern Recognition Letters, **15**(2):169–175, 1994.

Contact

Nicolas Passat
mail: passat@dpt-info.u-strasbg.fr
web: https://dpt-info.u-strasbg.fr/~passat
Jean-Paul Armspach
mail: armspach@ipb.u-strasbg.fr
web: http://www-ipb.u-strasbg.fr/staff/armspach